Available online at www.sciencedirect.com

ScienceDirect

Energy Procedia 00 (2016) 000–000

Energy Procedia

www.elsevier.com/locate/procedia

71st Conference of the Italian Thermal Machines Engineering Association, ATI2016, 14-16 September 2016, Turin, Italy

Numerical and Experimental Performance Analysis of Evaporative Condensers

Maria Fiorentino[a], Giuseppe Starace[b,*]

[a]*Decsa S.r.l., Via Cappelletta, Voghera 27058, Italy*
[b]*Department of Engineering for Innovation, University of Salento, Via per Monteroni, Lecce 73100, Italy*

Abstract

The heat rejection of industrial plants is often made with evaporative condensers as their choice meets energy efficiency requirements. In this work some numerical simulations of the evaporative condenser heat and mass transfer processes were carried out at the tube scale: 2D and 3D approaches were performed using the Ansys Fluent R.16.2 (VOF model). The time resolved characteristics of the film flow process were studied and two different types of flow (stable film and drops mode) were investigated, by varying the water-to-air mass flow ratio.
The decrease of the water-to-air mass flow ratio was found that led to the film break-up into droplets.
An experimental test rig was designed and built up for future validation works and to give designers new relations to quantify heat transfer performance depending on real working conditions.

Keywords: Evaporative condensers; Numerical Analysis; Flow Modes; Condenser test rig

1. Introduction

The heat rejection of industrial plants is often made with evaporative condensers where the refrigerant condenses in staggered tubes, whose outer surface is wet by falling water, while air flows upward.
The simultaneous heat and mass transfer processes improve the heat removal from refrigerant to air. The main advantages of the evaporative condensers are the following:

- the air flow rate required by an evaporative condenser is lower than that required by an air cooled condenser;

* Corresponding author. Tel.: +39 0809645195; fax: +39 1782745616.
E-mail address: giuseppe.starace@unisalento.it

Nomenclature

COP	Coefficient of Performance
d_{ext}	Tube outer diameter [mm]
D_{wa}	Water vapour diffusion coefficient to air [m^2s^{-1}]
F	Volume force [$N\cdot m^{-3}$]
G_M	Surface molar velocity of air [$kg\cdot mole\cdot m^{-2}\cdot s^{-1}$]
H	Enthalpy [$J\cdot kg^{-1}$]
k_G	Molar transfer coefficient [$kg\cdot mole\cdot Pa^{-1}m^{-2}s^{-1}$]
k_{eff}	Effective thermal conductivity [$W\cdot m^{-1}K^{-1}$]
k_m	Mass transfer coefficient from liquid water to vapour [$kg\cdot m^{-3}s^{-1}$]
L_t	Tube length [m]
$\dot{m}_{w,v}$	Mass transfer from water to vapour [$kg\cdot s^{-1}$]
M	Molecular weight [$kg\cdot kmol^{-1}$]
N_A	Water molar flux [$kg\cdot kmol\cdot m^{-2}s^{-1}$]
P_l	Longitudinal pitch [mm]
P_t	Transversal pitch [mm]
Re	Reynolds number [-]
S	Energy source term [$W\cdot m^{-3}$]
Sc	Schmidt number [-]
t	Time [s]
v	Velocity [$m\cdot s^{-1}$]]
x	Specific humidity [$kg\cdot kg_{da}{}^{-1}$]
z	Spatial coordinate along the tube length direction [m]
Greek symbols	
α	Volume fraction [-]
μ	Dynamic viscosity [$Pa\cdot s$]
ρ	Density [$kg\cdot m^{-3}$]
Subscripts	
atm	Atmospheric
da	Dry air
ma	Moist air
sat	Saturation
v	Vapour
w	Water

- the driving force of evaporative condensers is the difference between the condensing and the wet but temperatures. For this reason, compared to air cooled condensers, evaporative condensers reject the same amount of heat at lower condensing temperatures, resulting in a higher COP of the refrigeration plant they are operated in;
- the costs of water pumping are lower than that associated to water cooled condenser combined with a cooling tower.

Water evaporation to air makes the study of evaporative condensers very hard: many researchers [1] have dealt with their modeling. Parker and Treybal [2] suggested a design method for countercurrent evaporative coolers, based on Merkel hypothesis (Lewis number equal to unity), taking into account the water temperature variations.

Mizushina [3] obtained empirical correlations for heat and mass transfer coefficients of evaporative coolers. Kreid [4], Leidenfrost and Korenic [5] studied finned evaporative condensers. Bykov et al. [6] investigated heat and mass transfer as well as fluid flow characteristics in evaporative condensers, detecting complex patterns of water temperature and air enthalpy changes. Webb [7] proposed a unified mathematical model for cooling towers, evaporative coolers and condensers. Erens and Dreyer [8] compared empirical correlations provided by different authors to determine heat and mass transfer coefficients. They concluded that relationships provided by Mizushina [3] were valid over a wider range of operating conditions. Zalewski and Gryglaszewski [9] carried out theoretical analyses, based on Poppe work [10]. Ettouney [11] investigated the effect of condensing temperature and water-to-air mass flow rates ratio on evaporative condensers performance. Qureshi and Zubair [12] studied the influence of fouling on evaporative coolers and condensers performance. They introduced the fouling factor into the model developed by Dreyer [8]. Qureshi and Zubair [13] obtained an empirical relationship able to predict the water evaporation rate with a maximum error of 2%. In the most recent works the evaporative condensers were modeled at the tube scale.

Jahangeer et al. [14] and Islam et al.[15] developed a numerical model to investigate the heat transfer coefficients for a single straight tube wet by the water film and invested by air in a cross flow scheme and compared results with experimental data. In [16] Fiorentino and Starace modeled the evaporative condenser at tube scale with Ansys Fluent under stable film condition and compared the computed overall heat transfer coefficients values with those coming from empirical relationships.

In this work, the portion of fluid between two staggered tubes is modeled with Ansys Fluent and a constant wall temperature is assumed. The multiphase Volume of Fluid model is adopted and a purposely written down User Defined Function is used in order to calculate the moist air properties and the mass transfer coefficient from water to air.

The different flow modes are investigated and an experimental test rig is described that was signed and built up for future validations of computed results.

2. Mathematical model

The numerical model of an evaporative condenser would involve very high computational efforts if made at full scale over the entire thermo-fluid dynamic field of the unit.

For this reason a control volume was detected that consisted in the portion of fluid between two staggered straight tubes. These tubes are wet by falling water that creates a film over them; the air flows upward: the refrigerant is not modeled, since a constant temperature is assumed at the wall. The assumption of a uniform distribution of water by the feeding system leads to consider the vertical surfaces of the control volume as symmetric. The computational domain and the boundary conditions are represented in figure 1, while its geometrical characteristics are summarized in table 1. 2D and 3D numerical simulations were carried out.

The continuity (1), momentum (2) and energy (3) equations were solved using Ansys Fluent (Release 16.2) [17].

The multiphase model Volume of Fluid was adopted in order to track the position of water-to-air interface, where the mass and heat transfer phenomena take place. A scalar quantity, called "volume fraction" was associated to each phase and was calculated as the volume portion of the cell occupied by the phase. The sum of volume fraction corresponding to the different phases is equal to unity.

For the case study, the liquid and gas phases were represented by water and moist air, respectively.

$$\frac{\partial \alpha_w \rho_w}{\partial t} + \nabla \cdot (\alpha_w \rho_w \vec{v}_w) = \dot{m}_{w,v} \tag{1}$$

$$\frac{\partial}{\partial t}(\rho \vec{v}) + \nabla \cdot (\rho \vec{v} \vec{v}) = -\nabla p + \nabla \cdot [\mu(\nabla \vec{v} + \nabla \vec{v}^T)] + \rho \vec{v} + \vec{F} \tag{2}$$

$$\frac{\partial}{\partial t}(\rho H) + \nabla \cdot \big(\vec{v}(\rho H)\big) = \nabla \cdot \big(k_{eff} \nabla T\big) + S \tag{3}$$

The moist air was modeled as a mixture of dry air and water vapour. A C routine, named User Defined Function, was written down and loaded into the solver to define the thermo-physical properties of moist air and to model the water evaporation rate. The mass transfer coefficient was computed as follows.

Water vapor diffusion coefficient is obtained using the regression curve fit to the data [18]:

$$D_{w,a} = 10^{-6}(-2.775 + 4.479 \cdot 10^{-2} T_{ma} + 1.656 \cdot 10^{-4} {T_{ma}}^2) \tag{4}$$

The Schmidt number is:

$$Sc = \frac{\mu_{ma}}{\rho_{ma} D_{w,a}} \tag{5}$$

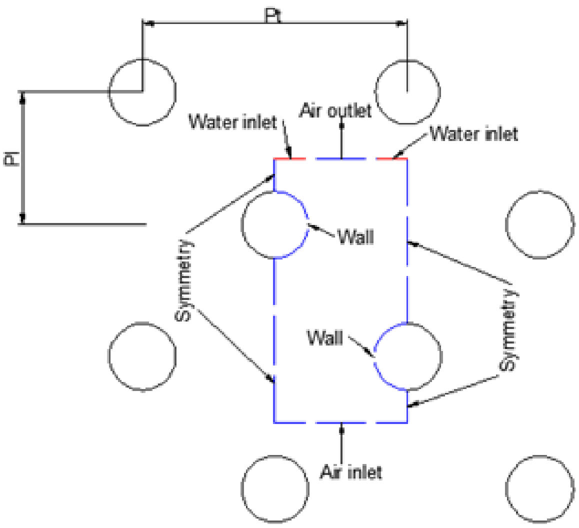

Figure 1. Computational domain and boundary conditions.

The surface molar velocity of air is defined as:

$$G_M = \frac{v_{ma}\rho_{ma}}{M_{ma}} \tag{6}$$

where the molecular weight of moist air is:

$$M_{ma} = \frac{M_{da}}{1 + 0.608 \cdot x_{ma}} \tag{7}$$

The molar transfer coefficient is defined as:

$$k_G = \frac{0.281 G_M}{p_{atm} Sc^{0.56} Re_{ma}^{0.4}} \tag{8}$$

The water molax flux depends on the difference between the saturation pressure evaluated at water temperature and vapour pressure in the air sorrounding the tube.

$$N_A = k_G(p_{v,sat} - p_v) \tag{9}$$

$$p_{v,sat} = exp\left(65.81 - \frac{7066.27}{T_w} - 5.976 ln T_w\right) \tag{10}$$

$$p_v = \frac{x_{ma} p_{atm}}{0.622 + x_{ma}} \tag{11}$$

The mass transfer coefficient that characterizes the water evaporation is calculates as:

$$k_m = N_A M_{ma} A_{interface} \tag{12}$$

The interfacial area density represents the area at the interface between water and air per unit mixture volume.

3. Grid and simulation settings

The 2D grid was made up of triangular elements while for 3D tetrahedral and hexahedral elements were adopted.

In order to better appreciate the liquid film thickness, the volume around the tube was meshed through boundary layer technique and the cells size was controlled by a size function. Actually a finer mesh was required near to the water-air interface, where the heat and mass transfer phenomena take place and the cells size increases with distance from the tube wall. The standard k-ε turbulence model was chosen for 2D simulations, while the SST k-omega model was used for 3D analyses. The SST model combines the k-ε in free stream and the k-ω near the wall. Wall functions were not used in the SST to reach a compromise of accuracy and acceptable computation times.

Table 1. Geometrical parameters of the computational domain.

	Unit	
d_{ext}	mm	25
P_l	mm	50
P_t	mm	100
3D simulations		
L_t	mm	180

4. Numerical results

The complete wettability of the heat transfer area ensures the correct operating of the evaporative condenser.

The temporal change characteristics of water flow were investigated in order to avoid the appearance of dry zones. The flow mode is influenced by the tubes arrangement (longitudinal and transversal pitch) and by the water-to-air mass flow ratio. The air and water mass flow rates corresponding to the different 2D testing cases are summarized in table 2.

The temporal change characteristics of film flow process for 2D studies are shown in figure 2.

The condition of stable film was reached at t=1.41 s for testing case A.

If the water mass flow rate decreases to 0.33 kg/s the liquid adheres to the tube wall and then breaks up into droplets at 1.34 s, since its momentum is not sufficient to avoid the rupture due to the countercurrent air resistance.

3D Simulations were carried out with the mass flow rates reported in table3. Figure 3 shows the 2D contours of water volume fraction corresponding to different values along the z-direction, at various times. Although the water is uniformly distributed at the inlet, the characteristics of the water flow change through the tube length.

Table 2. Water and air mass flow rates for 2D testing cases.

	Unit	Air mass flow rate	Water mass flow rate
Case A	kg/s	0.25	0.44
Case B	kg/s	0.25	0.33

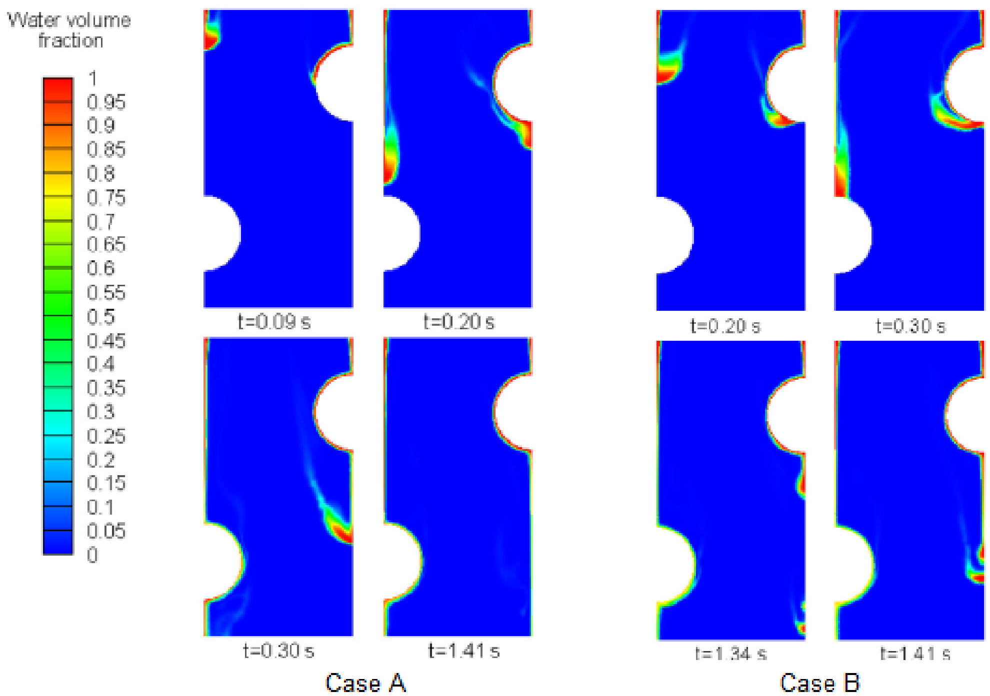

Figure 2. 2D temporal change characteristics of film flow process.

Table 3. Water and air mass flow rates for 3D simulation.

Unit	Air mass flow rate	Water mass flow rate
kg/s	0.015	0.09

5. Test rig description

The test bench (Fig.4) consists of:

- an air handling unit, equipped with a water chiller (condensed with air);
- the heat and mass transfer test section (designed both for tests on evaporative condensers and cooling towers heat transfer sections);
- the water circuit with heating system and temperature control;
- air ducts in a closed loop to connect the air handling unit and the test section;
- the connection between the cooling coils of the air handling unit and the water chiller.

5.1. Air handling unit

The air handling unit provides the air mass flow rate at given dry bulb temperature and relative humidity controlled at its outlet section. It consists of a water cooling coil, an electrical heating system and a high efficiency humidification (with water) section. The inverter fan is placed on the discharge of the air handling unit, together with an airflow meter.
The air is totally recirculated from the test section back to the handling unit. The air operating conditions are set by the user through a PID controller, placed on the board panel and the effective conditions are read on a display.

5.2. Heat and mass transfer section

The test chamber is a (450x200x1800 mm^3) made of four Plexiglas panels assembled with screws.

The heat transfer bank consists of eleven staggered tubes. Three of them are equipped with cartridge heaters with nominal power of 80W, in order to simulate the heat released by the refrigerant, and with thermo-resistances PT100, placed into a hole, able to read the temperature of tube outer surface. The superficial temperature is manually set by a temperature controller, by varying the load between 25 and 100 percent of the nominal one.

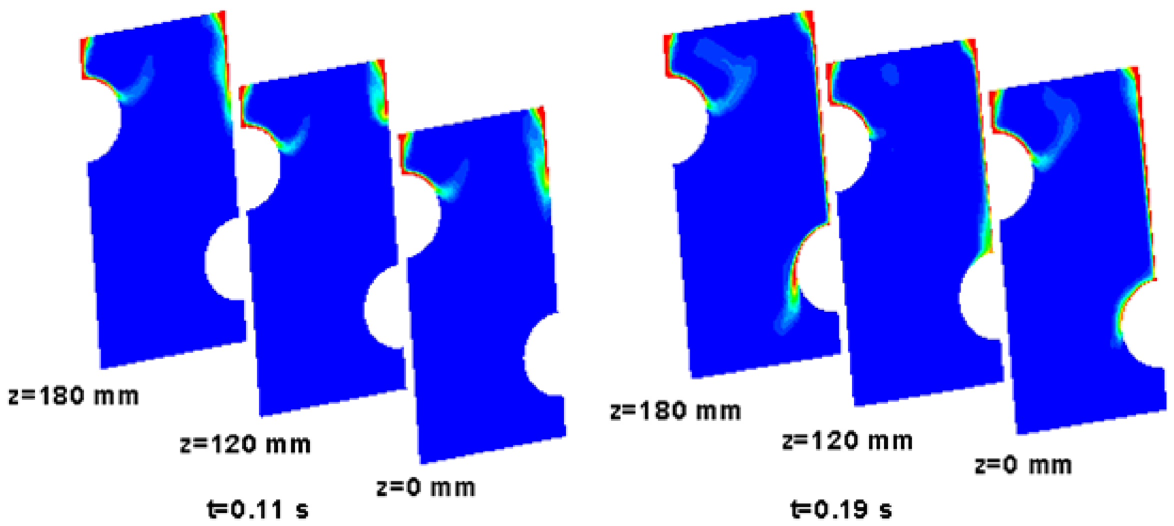

Figure 3. Water volume fraction variation along the z-direction.

The other tubes are used to establish the fluid flow. The tubes are mounted on two plates of Plexiglas, so that it's possible to vary their arrangement easily.

The water is provided by three distributor pipes placed in the upper part of the test chamber and a drop eliminator on the inlet of the air handling unit removes the water drops dragged by the air. The heat and mass transfer between the water and air at the outlet of the air handling unit takes place in the test section. Two thermo-hygrometers are used to measure the dry bulb temperature and relative humidity of air before and after its interaction with the electrical heaters, as can be seen in figure 4.

5.3. Water circuit

The water is taken from a basin below the test chamber and sent to the feeding system through a circulating pump, provided with an inverter that allows the flow regulation together with a 3-ways valve. The water mass flow rate is measured by an electromagnetic flowmeter. The water is heated by an electrical resistance heater in order to vary its temperature at the outlet of the PVC tubes within the range [10÷35] °C. The water level in the basin is controlled by a float valve, allowing the vaporized water make-up. A manual valve for the pipes drain is installed on the bottom of the basin.

5.4. Air duct

The connections between the air handling unit outlet and the test section and from the test section exit and the air handling unit inlet are made with metal ducts with a specific thickness to prevent vibrations and noise phenomena. They include curve portions and section restrictions to ensure a regular airflow.

5.5. Water chiller

The water chiller (condensed with air) with a capacity of 3 kW is equipped with a tank and a circulating pump. The pipelines between the cooling coil of the air handling unit and the water chiller are equipped with three-way valves in order to disconnect the circuit of the water-water heat transfer section. The temperature of the cooled water is controlled on the electric panel, while the airflow rate is regulated manually through a by-pass pipeline.

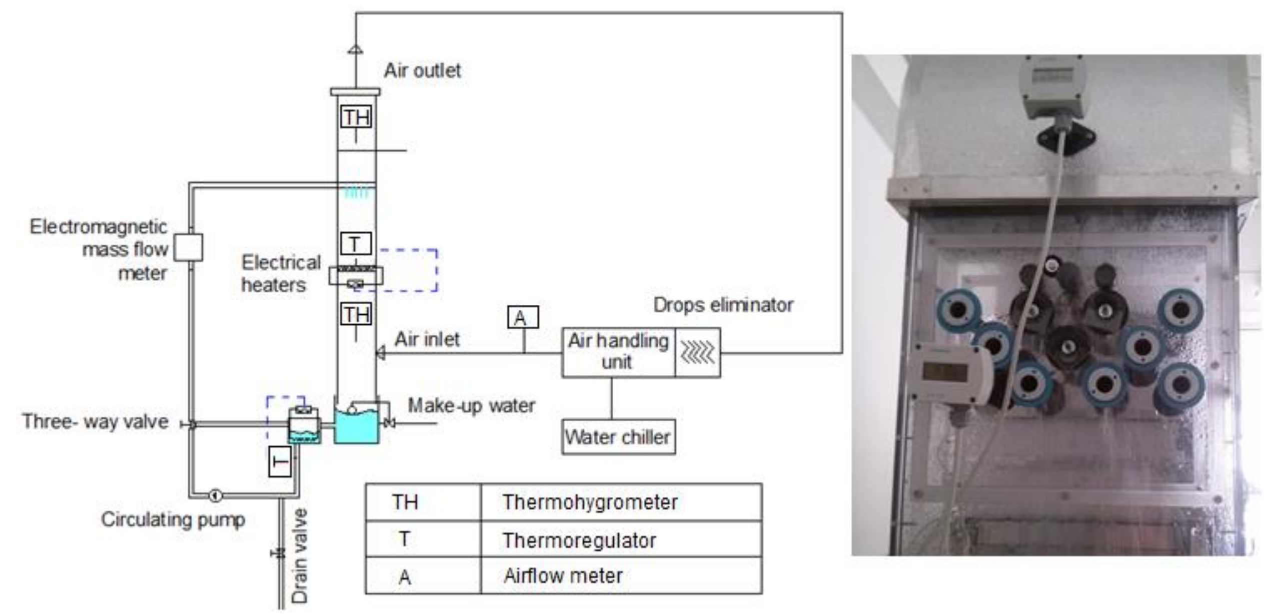

Figure 4. Working scheme of the experimental setup and details of the heat and mass transfer section.

6. Conclusions

The aim of this work was to present combined different approaches to study an evaporative condenser. The existing simplified mathematical models, compared to the numerical ones, evaluate the overall performance but do not allow to investigate aspects such as the water flow modes. The numerical simulation of the whole evaporative condenser involves high computational costs and for this reason the numerical analyses (both 2D and 3D) had to be carried at the tube scale, choosing a control volume consisting of the portion of fluid between two staggered tubes. The influence of the water mass flow rate was investigated: a decrease of 25% of the water-to-air mass flow ratio led to the film separation into droplets. The 3D simulations were useful to study the variation of the water film characteristics along the tube axis. The aim of this study was to find the most favorable operating conditions that ensure that the water flow covers the whole heat transfer geometry, especially the last rows that are furthest from the feeding point. The water mass flow rate will come from a compromise between the complete wettability of the heat transfer geometry and limited water pumping consumptions.

References

[1] Harby, K., Gebaly, D. R., Koura, N. S., and Hassan, M. S. "Performance improvement of vapor compression cooling systems using evaporative condenser: An overview." *Renewable and Sustainable Energy Reviews* 58 (2016): 347-360.

[2] Parker, R.O., and Treybal, R.E. The heat mass transfer characteristics of evaporative coolers, Chem. Eng. Prog. Symp. Ser. 57 (32) (1961) 138–149.

[3] Mizushina, T., Ito, R., and Miyashita, H. "Experimental study of an evaporative cooler." *International Chemical Engineering* 7.4 (1967): 727.

[4] Kreid, D. K., B. M. Johnson, and D. W. Failed. "Approximate analysis of heat transfer from the surface of a wet finned heat exchanger." *ASME paper* (1978).

[5] Leidenfrost, W., and Korenic, B. "Evaporative cooling and heat transfer augmentation related to reduced condenser temperatures." *Heat Transfer Engineering* 3.3-4 (1982): 38-59.

[6] Bykov, A. V., Gogolin, V. A., and Tovaras, N. V. "Investigation of heat, mass transfer and fluid flow characteristics in evaporative condensers." *International journal of refrigeration* 7.6 (1984): 342-347.

[7] Webb, R. L. "A unified theoretical treatment for thermal analysis of cooling towers, evaporative condensers, and fluid coolers." *ASHRAE transactions* 90.2 (1984): 398-415.

[8] Erens, J., and Dreyer, A. A. "An improved procedure for calculating the performance of evaporative closed circuit coolers." *The 25th National Heat Transfer Conference, Houston, AIChE Symposium Series*. Vol. 84. 1988.

[9] Zalewski, W., and Gryglaszewski, P. A. "Mathematical model of heat and mass transfer processes in evaporative fluid coolers." *Chemical Engineering and Processing: Process Intensification* 36.4 (1997): 271-280.

[10] Poppe, M., and Rögener, H. "Evaporative cooling systems." *VDI-Warmeatlas, Section Mh* (1984).

[11] Ettouney, H. M., El-Dessouky, H. T., Bouhamra, W., and Al-Azmi, B. "Performance of evaporative condensers" *Heat Transfer Engineering* 22.4 (2001): 41-55.

[12] Qureshi, B. A., and Zubair, S. M. "A comprehensive design and rating study of evaporative coolers and condensers. Part I. Performance evaluation." *International Journal of Refrigeration* 29.4 (2006): 645-658.

[13] Qureshi, B. A., and Zubair, S. M. "Prediction of evaporation losses in evaporative fluid coolers." *Applied thermal engineering* 27.2 (2007): 520-527.

[14] Jahangeer, K. A., Tay, A. A., and Islam, M. R. "Numerical investigation of transfer coefficients of an evaporatively-cooled condenser." *Applied Thermal Engineering* 31.10 (2011): 1655-1663.

[15] Islam, M. R., Jahangeer, K. A., and Chua, K. J. "Experimental and numerical study of an evaporatively-cooled condenser of air-conditioning systems." *Energy* 87 (2015): 390-399.

[16] Fiorentino, M., and Starace, G. "A Numerical Model to Investigate Evaporative Condensers Behaviour at Tube Scale." *ASME 2014 12th Biennial Conference on Engineering Systems Design and Analysis*. American Society of Mechanical Engineers, 2014.

[17] *ANSYS® Academic Research, Release 16.2, Help System, ANSYS, Inc.*

[18] R.E. Bolz, G.L. Tuve, CRC Handbook of Tables for Applied Engineering Science, second ed., CRC Press, 1973